The effects of cold production on seismic response

FEREIDOON VASHEGHANI and JOAN EMBLETON, University of Calgary, Canada

Cold production is a nonthermal recovery mechanism in which a progressive cavity pump simultaneously produces oil, water, gas, and sand.

This extraction decreases the reservoir pressure to values less than bubble point; therefore, gas comes out of solution and forms a foam-like material called foamy oil. On the other hand, due to sand production, high-porosity and high-permeability channels, known as wormholes, are created with diameters ranging from 10 cm to as much as 1 m (Tremblay et al., 1999).

It is very important to avoid drilling into the wormholes; therefore, petroleum engineers need to know the location of wormholes and the extent of depleted zones. Fortunately, the reservoir undergoes significant changes during cold production which we can monitor using seismic information. In this modeling study, we evaluate the influence of changes in porosity and foamy oil effects caused by cold production on seismic data.

Model and methodology

We used a simple three-layer homogeneous reservoir model with wormholes in the x and y directions and a vertical production well. This creates the L-shaped wormhole model shown in Figure 2. The top of the reservoir is at the depth of 200 m and reservoir is surrounded by overburden and underburden of constant properties. Modeling foamy-oil flow is based on some empirical adjustments to the solution-gas drive models (Maini, 2001). Some practical modifications are: critical gas saturation, oil/gas relative permeability, fluid and/or rock compressibility, pressure-dependent oil viscosity, absolute permeability, and bubble point pressure. We increased the critical gas saturation to 20% and modified the relative permeability curve for gas. Figure 1 shows the fluid properties used in the model.

There are two practical approaches for modeling wormhole behavior.

One method uses coupled geomechanical modeling. Fluid-flow equations are solved simultaneously with sand-flow relations. In each time step, the pressure field in the reservoir is calculated using the fluid-flow equations. The new pressure values are used in sand-flow equations to calculate the new porosity and therefore the permeability of each grid block. Then, in the next time step, the updated porosities and permeabilities are used to calculate the saturation and pressure and this loop continues until the desired results are achieved. This method is accurate but time-consuming and computationally expensive.

The other approach uses "static" wormholes in the reservoir—i.e., horizontal or other directional wells are used as wormholes. One major difference between these models is that static wormholes cannot be updated at each time step, so the reservoir specifications remain constant during the experiment. In this study we used two horizontal wells to represent the static wormholes in our model.

The black oil model is used in this study. Black oil simulation is a standard model which assumes that three components (oil, gas, and water) exist in the reservoir in three phases (liquid, free gas, and dissolved gas) and no change occurs in the composition of components during the life of the reservoir. We modeled production for 24 months at the rate of 500 b/d and the minimum bottom-hole pressure of 500 psi. Table 1 summarizes the simulation parameters. Figure 2 shows the plan view of the pressure in the reservoir after the simulation and a cross-section at x = 720 m. As expected, the pressure drop around the wormholes is higher than in other areas and explains the higher gas saturations around the wormholes. Figure 3 shows the plan view and a cross-section of gas saturation in the reservoir at x = 720 m.

Table 1: Reservoir Simulation Parameters

Reservoir size (m)	1010 × 1010 × 30
Simulation grid size (m)	10 × 10 × 10
Vertical well perforation (m)	30
Vertical well radius (m)	0.0762
Porosity (fraction)	0.3
Horizontal permeability (md)	2000
Vertical permeability (md)	200
Initial pressure (kPa)	3200
Temperature (°C)	35
Production time (days)	720
Min BHP (kPa)	500

Seismic modeling and imaging

The first step in our seismic modeling is calculating P-wave velocities for the reservoir using:

$$V_p = \sqrt{\frac{K + \frac{4}{3}\mu}{\rho}}$$

where K denotes the saturated bulk modulus, μ is saturated shear modulus and ρ is density. Density is given by the weighted average of fluid and matrix densities:

$$\rho = \varphi\,(S_o\rho_o + S_w\rho_w + S_g\rho_g) + (1-\varphi)\,\rho_m$$

where S denotes saturation and subscripts o, w, g, and m represent oil, water, gas, and matrix, respectively. The saturated shear modulus is constant and equal to the dry shear modulus; this means that fluids do not affect the shear properties of the reservoir.

$$\mu = \mu_{dry}$$

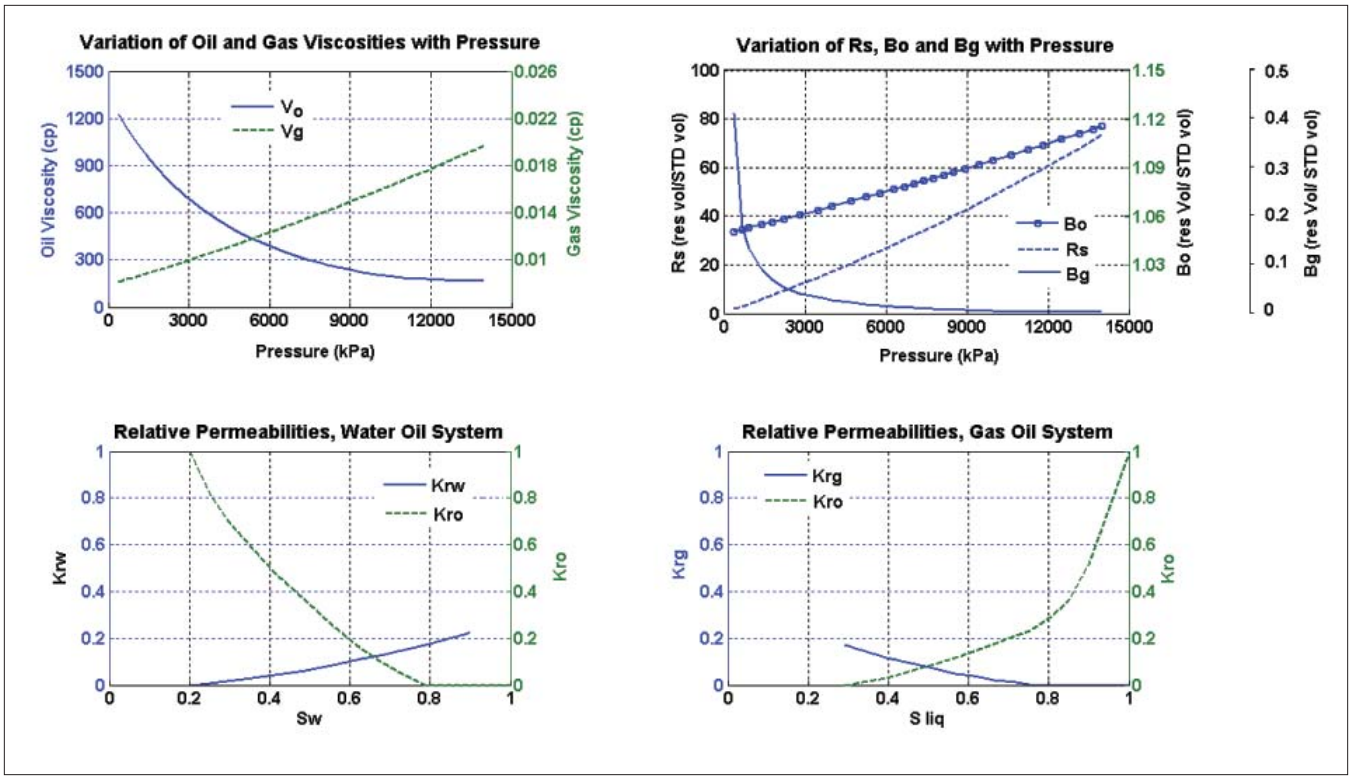

Figure 1. *Fluid properties. (top left) Oil and gas viscosities versus pressure. (bottom left) Oil and water relative permeabilities in a water-oil system versus water saturation. (top right) Variation of dissolved gas, oil, and gas-formation volume factors with pressure. (bottom right) Gas and oil relative permeabilities versus oil saturation in a gas-oil system.*

where μ_{dry} is the dry frame shear modulus of the rock. To calculate the saturated bulk modulus, we used Gassmann's equation:

$$K = K_{dry} + \frac{\left(1 + \frac{K_{dry}}{K_m}\right)^2}{\frac{\varphi}{K_f} + \frac{1 - \varphi}{K_m} + \frac{K_{dry}}{K_m^2}}$$

K_{dry}, K_m, and K_f are dry, matrix, and fluid bulk modulus, respectively, and φ is porosity. One important parameter is dry bulk modulus. Toksöz et al. (1976) defined the dry bulk modulus as

$$K_{dry} = K_m \left(\frac{1 - \varphi}{1 + \frac{3K_m\varphi}{4\mu_m}} \right)$$

This means that, if the porosity is constant, the dry bulk modulus will remain constant.

K_f, on the other hand, varies with pressure, temperature, and fluid saturation. Depending on the fluid distribution in the porous media, we can use either the harmonic or arithmetic average to calculate the overall bulk modulus of the reservoir fluids. Since we are dealing with foamy oil, the gas is distributed uniformly in the reservoir and we should use the harmonic average (Kirstetter et al., 2006):

$$\frac{1}{K_f} + \frac{S_o}{K_o} + \frac{S_w}{K_w} + \frac{S_g}{K_g}$$

Figure 4 shows the velocity maps calculated for the reservoir. P-wave velocity is very sensitive to changes in gas saturation and, even in zones with minimal changes in gas saturation, we observe a significant drop in velocity.

The P-wave seismic response was calculated by solving the 3D acoustic wave equation using a finite-difference scheme with second order accuracy in time and fourth order accuracy in space. The grid spacing, time steps, and dominant frequency are selected to keep the solution stable and grid dispersion is minimal. To avoid dispersion we used at least five grids per wavelength (Alford et al., 1976). To achieve a stable solution, we used the following relation (Lines et al., 1999):

$$\frac{v\Delta t}{h} \le \frac{1}{2}$$

where v is the seismic wave velocity, h is the spatial grid spacing, and Δt is the time increment. A damping zone at the boundaries prevented reflections off the nonphysical boundaries of the grid. Reverse-time depth migration is used for the imaging. Figure 5 shows the seismic results after the production.

Comparison of images generated by the modeling and reservoir simulation (Figures 2, 3, and 5) reveals that the

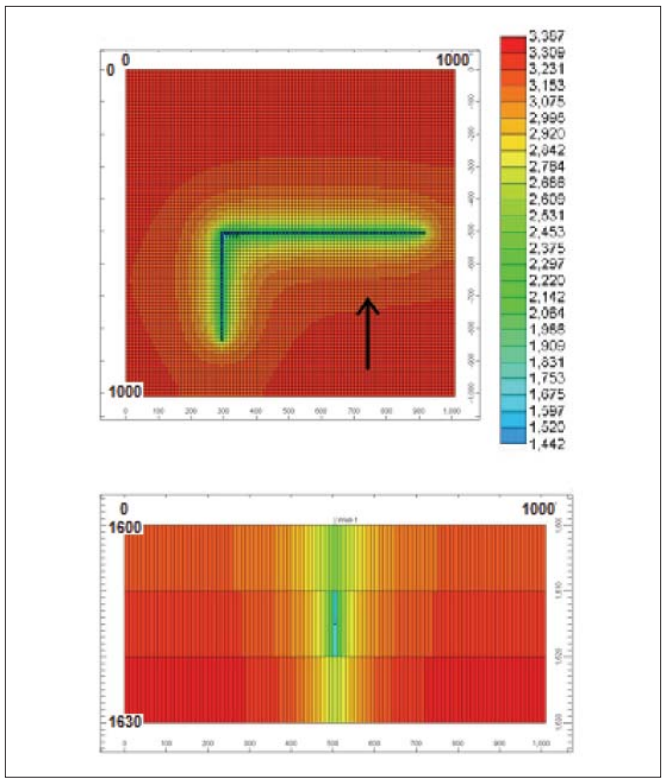

Figure 2. *Pressure in the reservoir. (top) Plan view of the middle layer. (bottom) Cross-section at x=720 m. The shape on the plan view is in the form of the letter L because two wormholes are in the x and y directions. The arrow shows the extent of the foamy oil zone (low-pressure zone).*

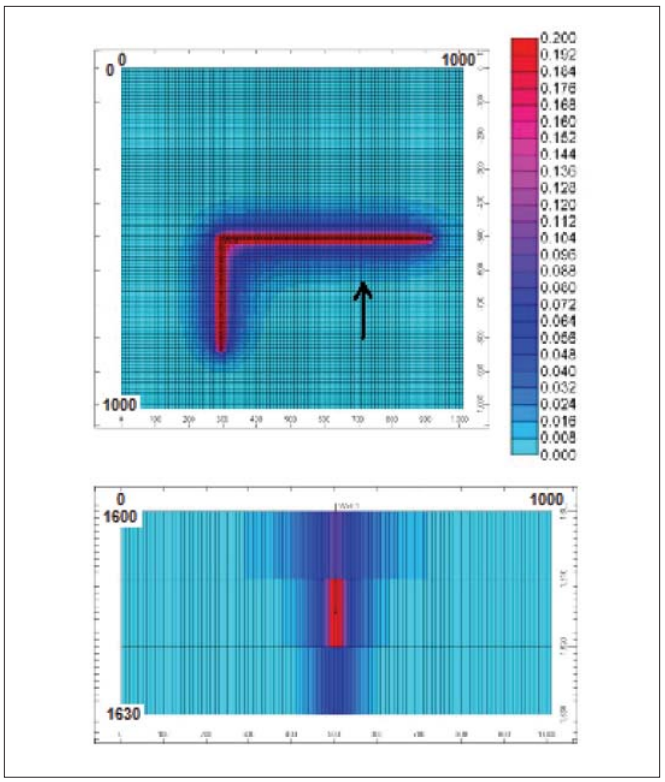

Figure 3. *Gas saturation in the reservoir. (top) Plan view of the middle layer. (bottom) Cross-section at x=720 m. The arrow shows the extent of the foamy oil zone (high gas-saturation zone).*

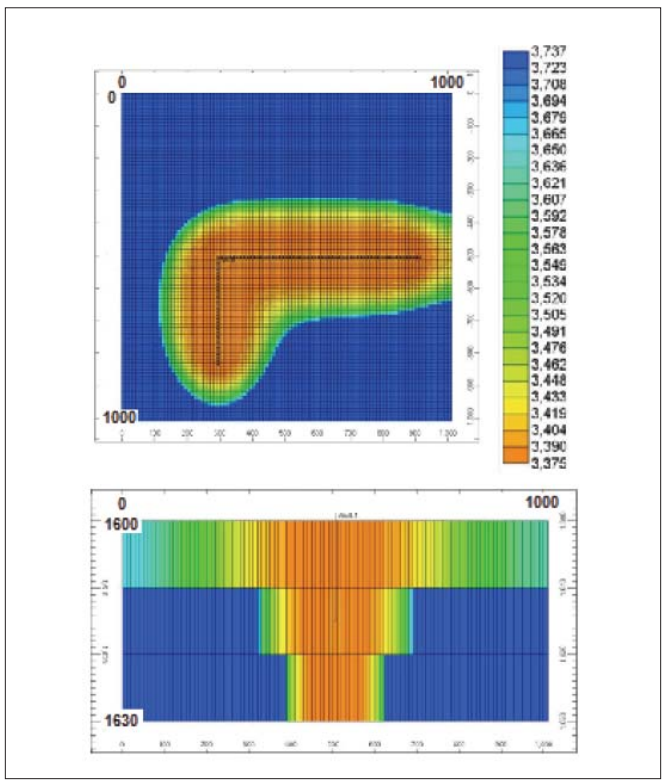

Figure 4. *Velocity maps of the reservoir calculated using Gassmann's equation. (top) Plan view. (bottom) Cross-section at x=720 m.*

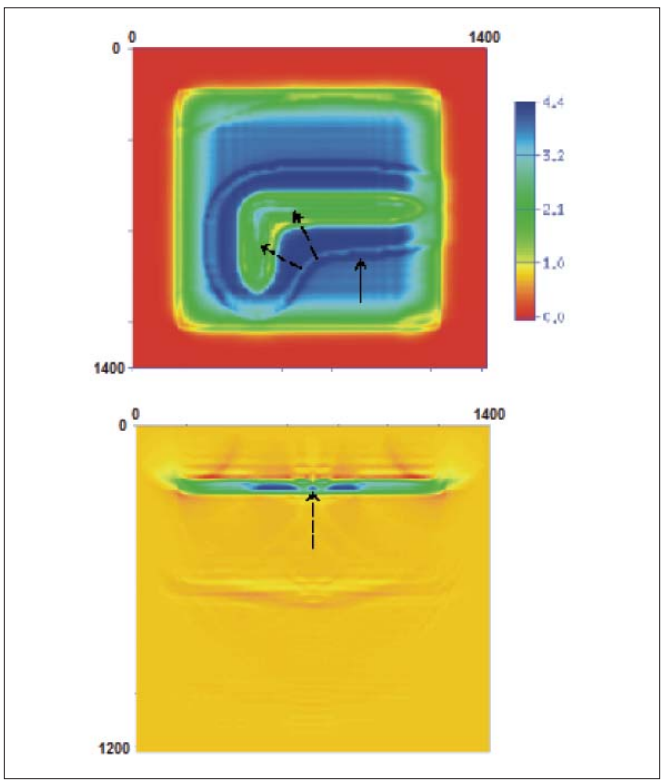

Figure 5. *Seismic response of the reservoir, depth-migrated. (top) Plan view. (bottom) Cross-section at x=720 m. Solid arrow shows the extent of the foamy oil zone. Wormholes are indicated by dashed arrows.*

extent of the foamy oil is indicated on the seismic response (solid arrows on the figures). However, the sizes of the zones on these maps are not equal. This is because even a very small change in the gas saturation dramatically decreases compressional-wave velocity (Domenico, 1976). On the other hand, the change in porosity caused by sand production does not have as much effect on the seismic response as expected. This is because the wormhole size is orders of magnitude less that the resolving power of conventional seismic surveys. However, the combined effects of gas saturation, pressure, and porosity at grid points around the wormholes can help us find an approximate location of the wormholes (dashed arrows on Figure 5).

Conclusions

Cold production of heavy oils creates foamy oil and wormholes in the reservoir and, for optimum recovery, it is very important to define these zones. Although the exact location of individual wormholes cannot be determined, we can find the approximate vicinities on seismic maps. This will help the engineers find the best locations for infill wells.

Suggested reading. "Accuracy of the finite-difference modeling of the acoustic wave equation" by Alford et al. (GEOPHYSICS, 1974). "Effect of brine-gas mixture on velocity in an unconsolidated sand reservoir" by Domenico et al. (GEOPHYSICS, 1976). "Elasticity/saturation relationships using flow simulation from an outcrop analogue for 4D seismic modeling" by Kirstetter et al. (*Petroleum Geoscience*, 2006). "A recipe for stability of finite-difference wave-equation computations" by Lines et al. (GEOPHYSICS, 1999). "Seismic pursuit of wormholes" by Lines et al. (*TLE*, 2003). "Seismic detection of cold production footprints in heavy oil extraction" by Lines and Daley (*Journal of Seismic Exploration*, 2007). "Foamy oil flow" by Maini (SPE paper 68885, 2001). "Velocities of seismic waves in porous rocks" by Toksöz et al. (GEOPHYSICS, 1976). "A review of cold production in heavy oil reservoirs" by Trembley et al. (10th European Symposium on Improved Oil Recovery, 1999). TLE

Acknowledgements: We would like to give our special thanks to Larry Lines for his valuable scientific and technical contributions to this work. The authors also thank the Consortium of Heavy Oil Research by University Scientists (CHORUS) and its sponsors for their technical and financial support. We appreciate the contributions from Alberta Ingenuity Centre for In Situ Energy (AICISE).

Corresponding author: vashegha@ucalgary.ca